
CHAPTER 3

PULSED LASER DEPOSITION OF OXIDES

3.1 Introduction

As a materials processing technique, laser ablation was utilized for the first time in the 1960's, after the first commercial ruby laser was invented¹. Nevertheless, as a thin film growth method it did not attract much research interest until the late 1980's², when it has been used for growing high temperature superconductor films. Since then, the development of the pulsed laser deposition (PLD) technique has been more rapid and the amount of research devoted to this topic has increased dramatically.

The advantages of PLD are the simplicity and versatility of the experiments. By using high-power pulsed UV-lasers and a vacuum chamber, a variety of stoichiometric oxide films can be grown in a reactive oxygen background gas without the need for further processing.

This chapter is mainly based on Chrisey and Hubler's book on "Pulsed Laser Deposition of Thin Films"³.

3.2 Chronological Development of PLD

1916 - Albert Einstein postulates the stimulated emission process

1960 - Theodore H. Maiman constructs the first optical maser using a rod of ruby as the lasing medium.

1962 - Breech and Cross use a ruby laser to vaporize and excite atoms from a solid surface.

1965 - Smith and Turner use a ruby laser to deposit thin films (this marked the very beginning of the development of the pulsed laser deposition technique).

Early 1980's - marked the creation of the first technological installation for laser deposition and epitaxy. A few research groups (mostly in the former USSR) achieved remarkable results on manufacturing thin-film structures using laser technology.

1987 - PLD was successfully used to grow high-temperature superconducting films.

Late 1980's - PLD as a film growth technique attained reputed fame and attracted wide spread interest; in particular, it was employed to fabricate crystalline thin films with epitaxy quality. Also the growth of ceramic oxide and nitride films, metallic multilayers and various superlattices by PLD were demonstrated.

1990's - brought rapid development of laser technology, which made PLD more competitive.

Lasers having a higher repetition rate than the early ruby laser made the thin film growth possible. Subsequently, reliable electronic Q-switched lasers became available for generation of very short optical pulses. For this reason, PLD can be used to achieve congruent evaporation of the target and to deposit stoichiometric thin films. Subsequent development led to lasers with a high efficient harmonic generator and excimer lasers delivering UV radiation. From then on, non-thermal laser ablation of the target material became highly efficient. Using PLD to synthesise buckminsterfullerenes has also been reported.

2000's - Production-related issues concerning reproducibility, large-area scale-up and multiple-level have begun to be addressed. It might start up another era of thin film fabrication in industry.

3.3 The dis-/advantages of PLD technique

During PLD, many experimental parameters can be changed, which have a strong influence on film properties. Laser related parameters such as laser fluence, wavelength, pulse duration and repetition rate can be altered. The preparation conditions including target-to-substrate distance, substrate temperature, background gas composition and pressure, may also be varied, which all influence the film growth.

Several aspects of PLD are beneficial. It produces a highly forward-directed and confined plume of materials which can be deposited with less contamination than, say, the unconfined plasma in a sputter process. In addition, PLD is incredibly precise. It can deposit for example a film of YBCO that is one unit cell (1.2 nm) thick; experiments show that a single unit cell of YBCO is a superconductor. In complex multicomponent material deposition with conventional evaporation methods, the various cations come from different sources. To produce the right mixture in the deposited film, the rate of arrival of each

species must be monitored and controlled. This becomes especially difficult when large background gas pressures are used during the deposition. PLD does not require such monitoring because the composition of the film replicates the composition of the target. In most ion beam based techniques, the pressure of the background gas in the chamber puts severe limitations on the operating parameters. For electron-beam evaporation, the background gas pressure cannot exceed 10^{-4} mbar, and for sputtering the pressure determines the rate of atom ejection from the target surface.

In addition, different molecules require different background pressures for forming the correct phase. For instance, ZrO_2 films can be formed in vacuum, but $SrTiO_3$ requires an oxygen pressure of 5×10^{-2} mbar. With PLD, the background gas pressure does not affect the passage or absorption of the laser beam, and the same system can be used to fabricate thin films composed of many materials by simply changing the background gas pressure. For example, PLD systems have been adapted to deposition systems in which the background gas pressure equals 1 mbar and to molecular beam epitaxy systems in which the pressure can be as low as 10^{-10} mbar.

Making multilayer materials can also be done rather easily with PLD, because different targets can be positioned under the laser beam. This is generally done with a computer-controlled multi-target holder or carousel.

PLD is a good technique for depositing extremely pure films. In most processes, the film includes contaminants. For example, thermal and electron-beam evaporation use a container for the source material, and the fairly high temperatures needed to evaporate the source materials can also evaporate parts of the container, thereby contaminating the deposition process. In metal organic chemical vapor deposition (MOCVD), volatile organic molecules transport the desired cations from the source to the final destination, and fragments of the organic molecules can end up in the film.

There are some drawbacks about PLD naturally. One of the major problems is the splashing or the deposition of particulates on the film. Two main causes for particle formation during laser evaporation are the breakaway of surface defects under thermal shock and splashing of liquid material due to superheating of subsurface layers. Some methods have been developed to reduce splashing. One is using a mechanical particle filter that consists of a velocity selector that acts as a high-velocity pass filter to remove slow-moving particulates. The second is using targets of high density and smooth surface – one

effective improvement is to polish the target surface before each run. The third is using relatively low energy density or low deposition rate.

Another problem is the lack of uniformity over a large area of the plume, due to the narrow angular distribution of the plume that comes out from the target surface. However, this can be solved by rastering the plume onto the substrate by rotation and translation in an engineered large area scale-up. With industrial excimer lasers available today, deposition rates of more than 1 micron-cm²/s are possible, and this is a commercially viable deposition rate. Some PLD systems can already deposit a thin film on an 8-inch wafer. Moreover, the demand for improved electronics based on metal-oxide or other multicomponent thin films should accelerate the development of commercial-scale PLD systems.

3.4 Mechanism of PLD process

This section presents the current state of understanding of some of the fundamental physico-chemical aspects of pulsed laser ablation and deposition, viewed from the perspectives of, respectively, the target, the plume and the deposited film.

The pulsed laser ablation process is a very complex one. At a superficial level, ablation might be viewed simply as a rapid boiling of material within a localised interaction volume at, and close to, the surface of the target. When investigated more deeply, however, the hidden complexity soon becomes apparent. Much of this complexity is illustrated, schematically, in figure 3.1.

If a solid or liquid is irradiated with an intense laser beam, a small amount of material on the surface is vaporized and ejected away from the sample. This vapor is a collection of atoms, molecules, ions and electrons, the exact ratio and kinetic energy of which depend on the laser parameters (intensity, wavelength, pulse width) and to some degree on the target sample. If this vapor comes in contact with another surface it may recondense on the surface. Repeated pulses of laser light and subsequently repeated vapor plumes might build up material on the surface to form what is termed a thin film.

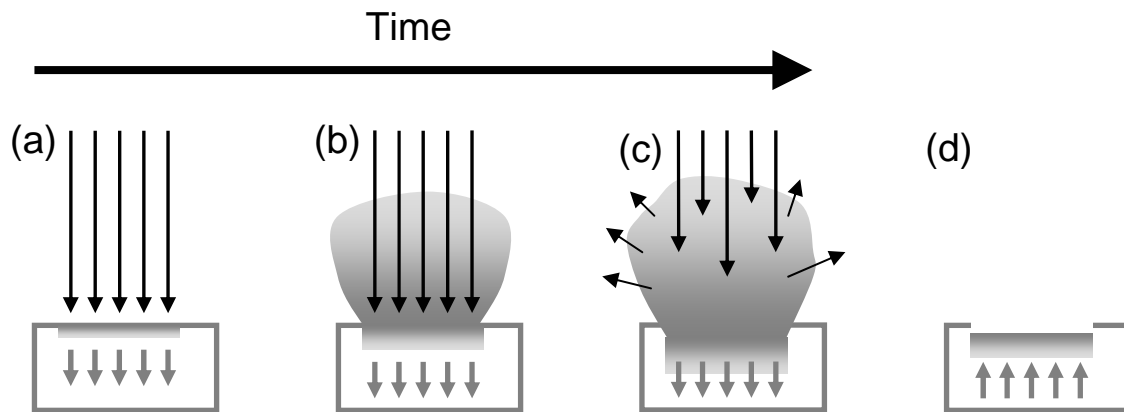


Figure 3.1 Schematic illustrating key elements of the pulsed laser ablation event. (a) Initial absorption of laser radiation (indicated by long arrows), melting and vaporization begin (shaded area indicates melted material, short arrows indicate motion of solid–liquid interface). (b) Melt front propagates into the solid, vaporization continues and laser-plume interactions start to become important. (c) Absorption of incident laser radiation by the plume, and plasma formation. (d) Melt front recedes leading to eventual re-solidification.

The growth and quality of the resulting film will generally depend on a number of fundamental parameters, including the choice of substrate, the substrate temperature, T_s , and the absolute and relative kinetic energies and/or arrival rates of the various constituents within the plume. The latter may be affected by the choice of excitation wavelength, by the laser pulse duration, energy and intensity, by the presence (or otherwise) of any background gas, and by any secondary plasma activation in the target–substrate gap.^{4,5}

The PLD process can be divided into the following steps and is shown schematically in figure 3.2:

1. Laser – target interaction
2. Plume expansion
3. Film deposition

Each step is very material dependent as well as dependent on experimental parameters such as laser wavelength, laser fluence and pulse width, background gas type and pressure, substrate type and temperature, and deposition geometry. Lasers used in PLD studies range in output wavelength from the mid infrared, *e.g.* a CO₂ laser, 10.6 μm , through the near infrared and visible, *e.g.* the Nd-YAG laser, with fundamental and second harmonic outputs at 1064 nm and 532 nm, respectively, down into the ultraviolet. Much current PLD work employs excimer lasers, which operate at a number of different UV wavelengths, *e.g.* 308 nm (XeCl), 248 nm (KrF), 193 nm (ArF) and 157 nm (F₂). Some typical parameters

for pulsed laser deposition are listed in Table 3.1 below.

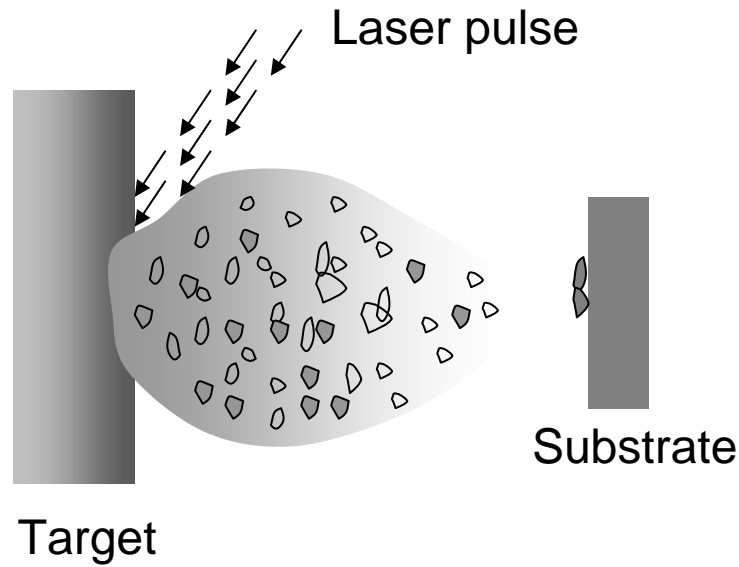


Figure 3.2 Schematic presentation of the pulsed laser deposition process.

Table 3.1 Typical parameters for pulsed laser deposition.

Parameter	Typical values
Materials examples	YBCO, BiSrCaCuO, BaTiO ₃ , ZnO, TiO ₂ ,...
Laser wavelength	193, 248, 266, 308, 355 nm, etc.
Laser pulse width	6 – 50 ns
Laser repetition rate	1 – 10 Hz
Laser fluence	0.5 – 5 J/cm ²
Vacuum pressure	... – 10 ⁻¹ mbar
Background gas	O ₂ , NO ₂ , H ₂ , Ar, etc.
Background gas pressure	1 – 300 mtorr
Substrate	MgO, SrTiO ₃ , Si, Al ₂ O ₃ , glass, etc.
Substrate temperature	25 – 800 °C

The time scales involved in the three process steps are very different. Typically, the laser-target interactions occur within nanoseconds, whereas the plume expansion in a background gas takes place within microseconds. Depending on the experimental conditions, the film growth process following a laser pulse can in principle continue to

develop until the next laser pulse occurs milliseconds later.

3.4.1 Laser – target interaction

We start by considering some of the mechanisms that can contribute to materials loss following irradiation of the target with pulsed photons (laser pulse). According to Kelly and Miotello⁶, these are generally divided into *primary* and *secondary* processes.

Suggested sub-divisions of the former include *thermal*, *electronic* and *macroscopic* sputtering, their relative importance depending on the nature of the target material and on the laser excitation wavelength and pulse duration; however, the distinctions between them are often not particularly clear-cut.

Direct evidence for *electronic* sputtering contributions in the case of metals and other extended solids is generally harder to discern, but reported examples include the observation of atoms with markedly non-thermal velocity distribution arising in laser-induced desorption from nano-sized metal particles⁷ and from thin metallic films⁸ (both findings have been attributed to surface–plasmon interactions), and even of graphite targets.⁹

Most detailed mechanistic considerations of target excitation and sputtering involve electronic initiation. Material interaction with an ultra-short laser pulse is assumed to involve very rapid excitation of the electron distribution, with efficient electron–electron coupling leading to an immediate rise in the electron temperature, subsequent heating of the lattice at a rate dependent upon the electron–phonon coupling strength, and eventual vaporization of the transiently heated target. *Electronic* contributions will thus tend to be most evident when using very short, *i.e.* sub-picosecond pulse durations, and can manifest themselves as unexpectedly large ion yields and/or supra-thermal propagation velocities within the expanding plasma plume.

Thermal contributions will generally dominate when using longer laser pulses, *e.g.* nanosecond pulses, of sufficient duration to allow photon coupling with both the electronic and vibrational modes of the target material. Such thermal contributions will be most favoured in cases where the target has low reflectivity, at the laser wavelength, a large absorption coefficient thus ensuring that the optical penetration depth is small, a low thermal diffusion coefficient and comparatively low boiling point, T_b . Since T_b will always

exceed the target melting temperature, T_m , evidence of wavelike structures on the post-irradiated target surface, indicative of localized melting, is often sought as confirmatory evidence for there being a thermal contribution to the ablation yield.

The material ejection mechanism and the total amount of ejected flux can change dramatically when the fluence increases sufficiently to induce explosive boiling of the target material. This process, sometimes referred to as phase explosion,¹⁰ occurs at temperatures approaching the critical point, T_c . It is viewed as an explosive relaxation of the laser induced melt into a co-existent mixture of liquid droplets and vapour. Such hydrodynamic ejection of droplet-like particulates is one illustration of *macroscopic* sputtering. Exfoliation, whereby macroscopic flakes detach from the target as a result of the repeated thermal shocks, is another example. This type of sputtering can arise when using target materials having high thermal expansion coefficients and a sufficiently high melting point that the thermal oscillations induced by repeated pulsed laser excitation do not exceed T_m . Macroscopic particulate ejection can also arise in the case of porous targets, wherein the localised laser induced heating will cause very rapid expansion of any trapped gas pockets just below the surface and forcible ejection of the surface material.

In contrast to ion bombardment, simple momentum transfer from an incident photon provides nothing like enough energy to dislodge an atom from the target surface. However, pulsed laser irradiation can lead to a number of indirect, or *secondary*, collision effects. Each ejected particle will have some velocity $v_x > 0$, where v_x is the velocity normal to the target surface. If the density of ablated material is sufficiently low, these particles will undergo collision-free expansion away from the interaction volume with a velocity distribution that is characteristic of the primary ablation process, *e.g.* a Maxwellian distribution in the case of a true thermal sputtering process. Clearly, this pulse of ejected material continues to expand but collisions in the early stages of the expansion, taking place in the Knudsen layer, are sufficiently frequent in order that the particle velocities approach equilibrium. The ensemble of particle velocities takes the form of a ‘shifted’ Maxwellian distribution:

$$P(v_x) \approx v_x^3 \exp\left[-\frac{m(v_x - u)^2}{2kT}\right] \quad (3-1)$$

where m is the particle mass. In other words, the distribution is forward peaked along x , with a positive flow velocity, u , but the individual particle velocities can span the entire

range $-\infty < v_x < +\infty$.

Some fraction of the ablated material is thus back-scattered towards the target surface; upon impacting the surface, these particles can induce secondary sputtering, be (elastically or inelastically) reflected or recondense. Such secondary encounters, which will affect an area much larger than the initial ablation spot, can have important consequences in the case of compound or multi-component targets. For example, the stoichiometry of the target surface will differ from that of the bulk if one or more of these surface collision events have a component dependent efficiency. This modified stoichiometry will then be reflected in the plume generated in any subsequent ablation event and, conceivably, in the composition of the deposited film. Such an explanation could account for the frequent observation that films grown by PLD from a multi-component target, in vacuum, are enriched in the less volatile component (*e.g.* Zn in the case of ZnO films).

Close inspection of target samples, post-ablation, often reveals a spectacular array of cone-shaped asperities. Such cone formation is frequently observed in targets that have been subjected to ion bombardment, and has been explained in terms of position dependent erosion probabilities such as might arise in the case of an inhomogeneous solid target, with sputter resistant ‘impurities’ surviving at the cone tips. By analogy, some authors have thus argued that cone formation observed in pulsed laser ablation must have similar origins, and that this provides evidence for secondary particle induced target sputtering. An alternative, and generally more widely accepted view, however, is that the cones arise from preferential ablation of all surface areas but those shielded by vaporization resistant inhomogeneities.¹¹ Such inhomogeneities may be naturally occurring, or laser induced. It is significant that many of the reported examples of laser induced cone formation have involved compounds, *e.g.* MgB₂ or YBCO, rather than elemental targets. Laser irradiation in such cases may induce localised changes in surface composition, due to preferential ablation or selective re-deposition of one constituent, and/or in morphology, *e.g.* the formation of resolidified or re-crystallised asperities, or by the re-deposition of ablation debris, that can serve as the ablation resistant nuclei that survive to become the tips of the eventual cones. The evident alignment of the cones, and the observation that their long axes are generally parallel with the propagation direction of the laser pulse, are both consistent with such a view.

Many reported laser ablation experiments are conducted in low pressures of background

gas rather than in vacuum. Clearly, new chemistry becomes possible given the presence of an appropriate background gas but, from the perspective of the target, the main effects of background gas will be to constrain the expansion of the plume of ejected material, higher gas phase number densities in the very early stages of plume expansion, and an enhanced probability of material re-deposition onto the target surface.

3.4.2 Plume expansion

This section attempts to characterize the formation, propagation, and properties of the plasma plumes typically encountered in PLD experiments, as revealed by numerous theoretical and mathematical modelling studies. As the plasma plume typically expands in vacuum or in a background atmosphere, we will treat separately the behaviour of the plasma plume for both experimental conditions.

Full characterization of the PLD plume requires an understanding of the advantages and limitations of several techniques. Despite the variety of diagnostic experiments designed to study PLD laser plumes, a number of major questions remain to be solved, including:

- * the role of nonthermal (electronic) and thermal (evaporation) ejection mechanisms in the ablation of material amounts necessary for film growth;
- * the extent and explanation of laser absorption by the initial ejectants;
- * the etching effects of the laser plasma on the target;
- * the expansion mechanism responsible for the high kinetic energy of the ejectants: the competition between adiabatic expansion and space charge acceleration models;
- * the fractional ionization of the plasma plume and the range of distances over which it can be electromagnetically steered;
- * the role of clusters and particulates in the mass transfer to the substrate;
- * the collision kinetics within the plume in the “collisionless” regime;
- * the role of scattering, diffusion, and hydrodynamics in the slowing and thermalization of the plume by background gases;
- * the major factors, i.e. kinetic energy, deposition rate, etc., determining the optimal film growth distance for various materials;
- * the role of chemistry with the background gas;
- * the role of target surface morphology and phase on the ejecta.

Plume expansion in vacuum

During a 30 ns PLD laser pulse in vacuum, a bubble of hot plasma is formed at approximately 50 μm from the target surface¹². As soon as the plasma is created, the plasma particles interact and tend to “lose memory” of the primary ablation mechanisms⁶. Thus, the plasma expansion can be described by certain characteristics, i.e. secondary ablation mechanisms¹² which to some extent are independent of the primary mechanisms. The expansion characteristics are described below:

i) Knudsen layer formation

Initially, the density of ablated particles may be high, in the range of $10^{18} - 10^{20} \text{ cm}^{-3}$, and the ablated particles close to the target surface have an anisotropic velocity distribution, all velocity vectors pointing away from the target surface. However, this anisotropic velocity distribution is transformed into an isotropic one by collisions among the ablated particles. This happens within a few mean-free paths from the surface, a region known as the Knudsen layer. It is mainly within this Knudsen layer that laser energy is absorbed in the plasma.

ii) High temperatures

Typical plasma temperatures measured by optical emission spectroscopy during the initial expansion are $\sim 10000 \text{ K}$, well above the boiling points of most materials ($\leq 3000 \text{ K}$).¹²

iii) Forward-directed plume

After the laser pulse has terminated, inter-particle collisions can lead to a highly anisotropic expansion of the plasma plume, which will typically be peaked in the forward direction, i.e. normal to the target surface. In a model by Singh and Narayan¹³, where they model the plasma as a fluid using the equations of gas dynamics followed by an adiabatic expansion, it is shown that during the incidence of the laser pulse, the isothermal expanding plasma is constantly augmented at its inner surface with evaporated particles from the target. The plasma is assumed to have exponential density gradients, and the velocity of various species vary linearly from the center of the plasma. The acceleration and the expansion velocities in this regime are found to depend upon the initial velocities of the plasma. Consequently, the highest velocities are obtained in the direction perpendicular to the target surface, where the initial plasma dimension is only tens of micrometers. Similar results emerge from the treatment by Anisimov *et al.*^{14,15}.

iv) High expansion velocities

At PLD conditions in vacuum, typical velocities of the particles in the leading edge of the plume are in the range of 10^4 m/s. For an ablated atom or ion with a mass of 100 amu, this corresponds to a kinetic energy of ~ 50 -200 eV. In general, ion velocities are higher than those of neutral species.

v) Complex plume

The plume composition is complex, especially for multicomponent targets, and may change during expansion. In the first few millimeters of the plume expansion, emission from atoms and ions, multiple charged ions and possible molecules can typically be observed together with Bremsstrahlung emission in the plasma. After the first millimeters of expansion, Bremsstrahlung emission and emission from multiple charged ions are no longer observed. In absorption spectroscopy ground-state atoms and ions have been observed in the plume after the initial expansion¹². Typically, non-emitting particles (i.e. ground-state atoms and ions) have broader velocity distributions than emitting particles at PLD conditions. The existence of fast neutrals in the plume can be explained by recombination of fast ions with electrons and/or resonant charge exchange between fast ions and neutrals. Electrons are more mobile than ions and neutrals, but are restricted from escaping the dense plasma by the strong space-charge field they build up by collectively moving away from the ions¹².

Plume expansion in a background atmosphere

Ambient gases present during PLD scatter, attenuate, and thermalize the plume, changing important film growth parameters such as the spatial distribution, deposition rate, and kinetic energy distribution of the depositing species. In addition, the plume particles can react chemically with the gas particles.

In general, raising the background pressure results in the following effects:

i) Increased fluorescence

An increase in fluorescence from all species due to collisions on the expansion front and subsequent interplume collisions compared with the expansion in vacuum can usually be observed¹².

ii) Sharpening of the plume boundary, indicative of a shock front

As the plume propagates into the background atmosphere it seems to push the background gas ahead and a sharp plume boundary may be created at the plume front. This plume sharpening indicates the formation of a shock front.

iii) Slowing of the plume

After a few microseconds of expansion and at sufficiently high background gas pressure, the plume slows down relative to the propagation in vacuum and eventually coalesces with slower moving material¹².

The velocity of the emitted particles is maximum for helium and minimum for argon background gas. This is attributed to larger degree of freedom per unit mass of helium than of any other gas and hence the collisional volume of helium is less as compared to that of other gases. The emitted species cover larger distances in helium atmosphere followed by air, oxygen, and argon. Misra and Thareja¹⁶ studied the ablation of an aluminium target by fast photography and found that particle's velocity is maximum in helium - 7.29×10^4 m/s, followed by air - 6.84×10^4 m/s, oxygen - 6.75×10^4 m/s and argon - 6.21×10^4 m/s, at a pressure of 10 mbar for laser energy of 100 mJ.

iv) Plume splitting

At intermediate background gas pressures (in the 10^{-3} mbar range) the plume tends to split up into a fast (collisionless) and a slow (scattered) component.

v) Changes in angular distribution

In the presence of an ambient gas, the nascent plume angular distribution is perturbed by additional plume particles collisions with the background gas. These collisions scatter the plume particles from their original trajectories and broaden the angular distribution.

Collision-induced broadening effects might be expected to begin appearing when the mean free path of a particle in the background gas starts to become less than the target-substrate distance, h . The particle mean free path, Λ , is roughly $(\sqrt{2}n\sigma)^{-1}$, where n is the number density of the gas (proportional to pressure) and σ is the collision cross section. For target-substrate distances in the centimeter range, experiments¹⁷ indicate that changes in angular distribution become significant when h/Λ is around 10.

vi) Plume thermalisation

With typical PLD target-substrate distances around a few centimeters and at sufficiently high background gas pressures, i.e. $\geq 10^{-1}$ mbar approximately, the plume particles can thermalise completely.

vii) Chemical reactions

Reactive scattering can result in the formation of molecules or clusters in the plume¹².

3.4.3 Film growth

Film growth processes, i.e. deposition of ejected target material onto a substrate, can be described by the following sequence: the arriving particles must adsorb on the substrate surface, after which they may diffuse some distance before they react with each other and the surface and start to nucleate. The way the particles nucleate may determine the structure or morphology of the growing film. Under certain circumstances, e.g. high substrate temperature, diffusional interactions within the film and with the substrate, beneath the growing film surface, may subsequently modify film composition and film properties.

In the following, some typical film growth modes will be briefly described and some PLD growth characteristics will be discussed, in particular different film structures will be mentioned. The following sub-sections are mainly based on the references^{18,19}.

Typical growth modes

In considering the general theory of film nucleation and growth, there are three conventional modes of nucleation and growth:

1. Three-dimensional island growth – the Volmer-Weber growth.
2. Two-dimensional full-monolayer growth – the Frank-van der Merwe growth.
3. Two-dimensional growth of full monolayers followed by nucleation and growth of three-dimensional islands – the Stranski-Krastinov growth.

The selection of one of these growth modes by a substrate-film system depends on (a) the thermodynamics that relates the surface energies of the film and substrate, and (b) the film-substrate interface energy.

i) Volmer-Weber Nucleation and Growth

Figure 3.3 illustrates the different processes involved in the nucleation of clusters on a surface by vapour deposition of atoms. Film atoms arrive at a rate dependent on the deposition parameters either on bare substrates areas or on preexisting clusters of film atoms. These film atoms can subsequently diffuse over the substrate or cluster surface, encounter other mobile film atom to form mobile or stationary clusters, attach to preexisting film-atom clusters, be reevaporated from the substrate or from a cluster, or be detached from a cluster and remain on the substrate surface.

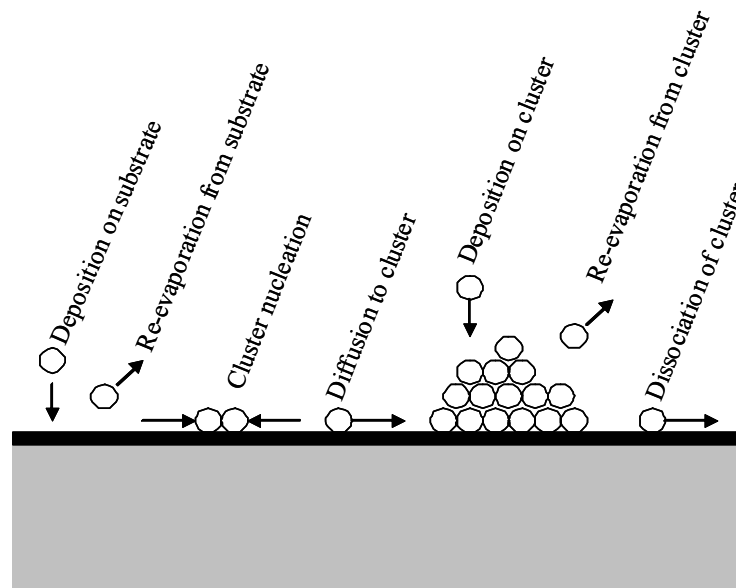


Figure 3.3 Schematic diagram of atomic processes in the nucleation of three dimensional clusters of deposited film atoms on a substrate surface.

The balance between growth and dissolution processes for a given cluster will be governed by the total free energy of the cluster, ΔG , relative to an assemble of individual atoms. For three-dimensional cluster growth, ΔG will have a maximum, ΔG^* , at a critical cluster size which means that cluster sizes above this critical size are stable.

To a first approximation *the nucleation rate* is given as the product:

$$[\text{arrival rate of atoms at critical-size nucleus}] \times [\text{concentration of critical nuclei}]$$

The first term is proportional to the concentration of mobile atoms on the surface and to the surface diffusion coefficient. The second term is a strongly decreasing function of ΔG^* . As

a rule, an increased cluster nucleation rate is desired in Volmer-Weber growth. In practice, this can be achieved by increasing the deposition rate or decreasing the substrate temperature, which gives a decrease in ΔG^* . Another possibility is to decrease the net surface/interface free energy (and thereby decrease ΔG^*), e.g. by creating interactions with a background gas.

ii) Frank - van der Merwe Nucleation and Growth

Full monolayer growth involves the nucleation and growth of islands that are only one monolayer thick and grow to essentially complete coalescence before significant clusters are developed on the next film layer. In this case there is no free energy barrier to nucleation, i.e. no ΔG^* . If the substrate material is different from the film material, full monolayer nucleation will be promoted by strong film-substrate bonding, low film surface energy and high substrate surface energy.

iii) Stranski-Krastinov Nucleation and Growth

Full monolayer growth may change to three-dimensional island growth after 1-5 monolayers due to a change in the energy situation with successive monolayers. This might be an increase in stress with increasing layer thickness due to mismatched lattice spacings.

Characteristics of PLD growth

Qualitatively, a possible event scheme for nucleation during a PLD cycle is as follows (assuming a high instantaneous vapour flux)¹⁸:

- * A vapour pulse causes the nucleation of a high density of small subcritical clusters, i.e. clusters that are much smaller than those that would be stable for a lower instantaneous deposition rate. The subcritical clusters are expected to be unstable once the vapour pulse has decayed after approximately 1 ms.
- * The subcritical clusters will tend to dissociate into mobile species.
- * The mobile species will nucleate new clusters on a different scale during the time of no vapour arrival - typically 100 ms (laser repetition rate of 10 Hz).
- * The next pulse will initiate the same sequence with some of the mobile atoms being added to the clusters formed following the first pulse.

If the atomic process time constants, T_{ap} , (i.e. the time constants for all the relevant diffusion, accumulation and dissociation phenomena) are much smaller than the period of the PLD cycle, T_{cycle} , the pulsed vapour arrival should not affect the final film result

significantly. However, if $T_{cycle} \approx T_{ap}$, then the film formation pattern may be altered.

If the PLD is performed in a background gas, e.g. oxygen, the background gas may promote stoichiometric film formation as oxide deposition. Furthermore, as mentioned above, the presence of a background gas may change film and substrate surface energies, possibly even the film growth mode. However, it is difficult to predict specific effects since they will depend on sticking coefficients, reaction rates and other factors.

According to Metev¹⁹, the two main thermodynamic parameters that determine film growth in PLD are the substrate temperature, T_s , and the supersaturation, m , where the latter is proportional to $T_s \times \ln(R_a/R_e)$. Here, R_a stands for the actual deposition rate and R_e is the equilibrium deposition rate at temperature T_s .

An increase in substrate temperature will increase, for instance, the rate of surface diffusion of the adsorbed particles. For typical PLD conditions, the actual deposition rate can be varied in a controlled manner by the experimental conditions over a wide range from $R_a \sim 10^{14}$ to 10^{22} cm⁻²s⁻¹.

Other important process parameters that may influence the film growth are the flux, the energy, the ionisation degree and the type of condensing particles.

Surely, the physicochemical properties of the substrate are essential for film growth as well. For example, YBCO films are typically grown on non-interacting, nearly lattice-matched crystalline substrates such as <100> MgO, SrTiO₃ and LaAlO₃¹⁸.

Structure development

The development of the deposited film structure changes with the amount of thermal motion that takes place during film growth and also with the amount of additional energy that is delivered to the growing surface as indicated above.

Important parameters are the ratio of the substrate temperature, T_s , to the melting point of the film, T_m (in Kelvin), and the distance between adsorption sites, a , compared with the diffusion length, ΛD , of the adsorbed particles. Four main structural zones have been identified in vapor-phase processes²⁰.

Zone 1: When T_s/T_m is so low that surface diffusion is negligible ($\Lambda D < a$), the film may consist of columns typically tens of nanometers in diameter separated by voids a few

nanometers across. The columns have poor crystallinity or are amorphous. In thicker films this structure may be superimposed with an array of cones with wider voids between them, which terminate in domes at the surface.

Zone T: This zone is usually associated with energy-enhanced processes such as in PLD. When $\Lambda D < a$, the film may contain defected columns similar to those of *zone 1*, but the voids and domes are absent.

Zone 2: When $T_s/T_m > 0.3$ approximately so that surface diffusion becomes significant, the film may consist of columns that have tight grain boundaries between them. The crystalline columns have less defects than in *zone 1* and *zone T* and are often faceted at the surface. This *zone* structure can also occur in amorphous films, where the plane boundaries are planes of reduced bonding rather than planes of crystallographic discontinuity.

Zone 3: For $T_s/T_m > 0.5$, considerable bulk annealing of the film is taking place during deposition, the film may under certain circumstances consist of more isotropic or equiaxed crystallite shapes. Film structures are often associated with smooth film surfaces. However, the grain boundaries can develop grooves.

In general, the “optimum” substrate temperature for high-quality thin-film growth is when $0.3 < T_s/T_m < 0.5$, where there is sufficient surface diffusion to allow surface atoms to minimise their surface energy, reaching thermodynamically stable sites.²⁰

Formation of particulates

One major problem in PLD is the presence of particulates on the film surface. Particulates can originate from liquid droplets that are expelled from the target during irradiation, from ejected protruding surface features that are mechanically removed from the target by laser-induced thermal and mechanical shock, or from cluster condensation from vapour species due to supersaturation²¹. The first particulate type is typically observed at laser power densities above 10^7 W/cm², and the latter type is most likely observed in the presence of a background gas during film deposition²¹. Typical particulate sizes are in the micron and submicron ranges, however, for particulates formed from the vapour state the size tends to be in the nanometer range. In general, the density and the size of particulates on the deposited film surface tend to increase with increasing laser fluence and with increasing

laser wavelength²¹. However, other process parameters such as laser spot size and ambient gas pressure are important as well.

3.5 Summary

PLD is a relatively simple experimental deposition technique. However, the deposition process is in fact rather complex and in order to deposit films of optimum quality, the process parameters must be controlled in an adequate manner. Process parameters such as the deposition rate, the kinetic energy of ablated particles and the mobility of adsorbed particles may be controlled by experimental parameters such as the laser fluence, the background gas pressure and the substrate temperature. The optimum process parameters, however, vary from one material to another.

PLD is a film growth technique which is interesting primarily for deposition of multicomponent oxide materials. Indeed, within this field, the technique is competitive to other vacuum deposition techniques.

3.6 References

1. H.M. Smith and A.F. Turner, "Vacuum deposited thin films using a ruby laser", *Appl. Opt.* 4 (1965) 147.
2. D. Dijkkamp, T. Venkatesan, X.D. Wu, S.A. Shaheen, N. Jisrawi, Y.H. Min-Lee, W.L. McLean and M. Croft, "Preparation of Y-Ba-Cu oxide superconductor thin films using pulsed laser evaporation from high T_c bulk material", *Appl. Phys. Lett.* 51 (1987) 619-621.
3. D.B. Chrisey and G.K. Hubler (Eds.), "Pulsed Laser Deposition of Thin Films", Wiley, New York, 1994.
4. P.R. Willmott and J.R. Huber, "Pulsed laser vaporization and deposition", *Rev. Mod. Phys.* 72 (2000) 315-328.
5. A. Giardini, V. Marotta, A. Morone, S. Orlando and G.P. Parisi, "Thin films deposition in RF generated plasma by reactive pulsed laser ablation", *Appl. Surf. Sci.* 197 (2002) 338-342.
6. R. Kelly and A. Miotello, "Mechanisms of pulsed laser sputtering", in ref. 3, pp.55-87.

7. W. Hoheisel, K. Jungmann, M. Vollmer, R. Weidenauer and F. Träger, “Desorption stimulated by laser-induced surface-plasmon excitation”, *Phys. Rev. Lett.* 60 (1988) 1649-1652.
8. I. Lee, J.E. Parks, T.A. Callcott and E.T. Arakawa, “Surface-plasmon-induced desorption by the attenuated-total-reflection method”, *Phys. Rev. B.* 39 (1989) 8012-8014.
9. D.J. Krajnovich, “Laser sputtering of highly oriented pyrolytic graphite at 248 nm“, *J. Chem. Phys.* 102 (1995) 726-743.
10. A. Miotello and R. Kelly, “Laser-induced phase explosion: new physical problems when a condensed phase approaches the thermodynamic critical temperature”, *Appl. Phys. A* 69 (1999) S67-S73.
11. D.J. Krajnovich, J.E. Vazquez and R.J. Savoy, “Impurity-driven cone formation during laser sputtering of graphite”, *Science* 259 (1993) 1590-1592.
12. D.B. Geohegan, “Diagnostics and characteristics of pulsed laser deposition laser plasmas”, in ref. 3, pp.115-165.
13. R.K. Singh and J. Narayan, “Pulsed-laser evaporation technique for deposition of thin films: Physics and theoretical model”, *Phys. Rev. B* 41 (1990) 8843-8859.
14. S.I. Anisimov, D. Bäuerle and B.S. Luk'yanchuk, “Gas dynamics and film profiles in pulsed-laser deposition of materials”, *Phys. Rev. B* 48 (1993)12076-12081.
15. S.I. Anisimov, B.S. Luk'yanchuk and A. Luches, “An analytical model for three-dimensional laser plume expansion into vacuum in hydrodynamic regime”, *Appl. Surf. Sci.* 96-98 (1996) 24-32.
16. A. Misra and R.K. Thareja, “Investigation of laser ablated plumes using fast photography”, *IEEE Transactions on Plasma Science*, 27 (1999) 1553-1558.
17. K.L. Saenger, “Angular distribution of ablated material”, in ref. 3, pp.199-227.
18. J.S. Horwitz and J.A. Sprague, “Film nucleation and film growth in pulsed laser deposition of ceramics”, in ref. 3, pp.229-254.
19. S. Metev, “Process characteristics and film properties in pulsed laser deposition”, in ref. 3, pp.255-264.
20. G.K. Hubler, “Comparison of vacuum deposition techniques”, in ref. 3, pp.327-355.
21. L.C. Chen, “Particulates generated by pulsed laser ablation”, in ref. 3, pp.167-171.